Original research article

A modified mode-mismatched thermal lens spectrometry Z-scan model: An exact general approach

Abdul Rahman [a,b,*], Kulsoom Rahim [c], Imrana Ashraf [a,b], Humberto Cabrera [a,*]

[a] *Optics Lab, STI Unit, The Abdus Salam International Centre for Theoretical Physics (ICTP), Strada Costiera 11, Trieste, 34151, Italy*
[b] *Department of Physics, Quaid-i-Azam University, Islamabad 45320, Pakistan*
[c] *Department of Basic Sciences, University of Engineering and Technology, Taxila 47080, Pakistan*

ARTICLE INFO

ABSTRACT

In this work we introduce a modified pump-probe mode-mismatched thermal lens Z-scan theoretical model for measurement of thermo-optical properties including absorption coefficient and thermal diffusivity of semitransparent liquids. We present an exact solution for the theoretical thermal lens (TL) signal which agrees pretty well with the experimental one under different experimental configurations. The TL signal as a function of the detector position (L) has been analyzed using the pinhole size (ρ_0) as a critical parameter. We illustrate its validity by calculating the TL signal in Z-scan experiment and situation with small and large values of L as well as measuring the absorption coefficient and thermal diffusivity of water.

1. Introduction

Thermal lens spectroscopy is a highly sensitive optical method widely used for measurement of absorption coefficient and photothermal parameters of semi-transparent samples [1–5]. It is based on the use of the thermal lens (TL) effect generated by the spatially dependent temperature distribution induced in a sample following the absorption of an excitation laser beam [6–10]. The probing laser beam passes through the sample and its phase is affected by the TL effect thus producing a divergent or convergent beam depending on the nature of the material. By measuring the variation of the probe beam intensity at the detector position, the TL signal can be measured and processed. The magnitude of the TL signal depends on photothermal parameters including the excitation power and the amount of light absorbed by the irradiated sample, which depends on the absorption coefficient. Previously developed theoretical models, to study TL signals, were based on Fresnel-diffraction approximation, for situations in which the sample is located at a fixed position [11]. Later on, Marcano et al. [12] developed a model for Z-scan experiment based on the same approximation, which also includes the aberration nature of the TL. This model successfully describes the behavior of the TL signal generated in an experimental configuration based on focused excitation and collimated probe beams and measuring the transmission of probe light through a small aperture. They claimed an excellent agreement between theoretical and experimental values when performing Z-scan experiments for specific case in which the radius of aperture (ρ_0) was ignored. However, in their results, the values of L are very large (2000 cm) in order to match the theoretical and experimental TL signals, which is cumbersome in real experimental configuration. Because of that, in more general cases it is necessary to consider the influence of ρ_0 on the TL signal which presents uncertainties if L is too small.

In our proposal we expand previous TL model including ρ_0 and the distance between sample and detector (L) as well as considering real situations in which L takes large and short values. In both cases, our results essentially show pretty good matching

---

* Corresponding author at: Optics Lab, STI Unit, The Abdus Salam International Centre for Theoretical Physics (ICTP), Strada Costiera 11, Trieste, 34151, Italy.
E-mail addresses: abdulrehmanqau.phy@gmail.com (A. Rahman), hcabrera@ictp.it (H. Cabrera).
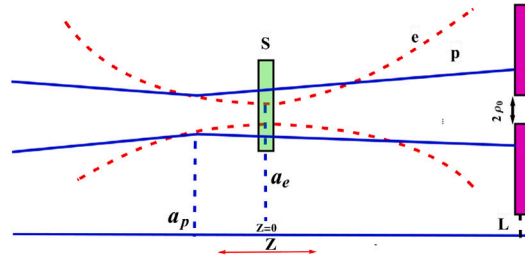
Fig. 1. Schematic diagram of mode-mismatched TL Z-scan. Here p, e, a_p, a_e are probe beam, excitation beam, beam waist positions of probe and excitation beam respectively. a_e is fixed at the origin of coordinate system $Z = 0$. Distance of the detector from origin $Z = 0$ is L, whereas sample to detector distance is $\zeta = L - z$ with $Z = 0$ in Z-scan experiment.

between the theoretical and experimental values. The paper is organized as follows. In section (II) we present the exact analytical theory for Z-scan experiment in far field approximation and discuss theoretical results in mode- mismatched configuration with the exact solution which includes ρ_0 and L dependences. In section (III) we perform Z-scan experiment with water and compare results of absorption coefficient and thermal diffusivity values obtained using different TL models.

2. Modified theoretical model: general solution

In our calculation, we have considered the dual-beam mode-mismatched TL experimental configuration proposed by Marcano et al. [12] as shown in Fig. 1. The position of the sample is taken as the origin of coordinate system ($Z = 0$). Following the same procedure used in [11,12], the expression for the probe beam electric field amplitude after being distorted by the TL effect, is calculated at the detector plane by the following expression,

$$U(r, z, t) = \frac{i}{\zeta \lambda_p} exp\left\{\frac{-2i\pi}{\lambda_p}\left(\zeta + \frac{r^2}{2\zeta}\right)\right\} \int_0^{2\pi} \int_0^\infty U_i(r_1, z, t)$$
$$exp\left\{\frac{-i\pi}{\lambda_p}\frac{r_1^2}{\zeta}\right\} exp\left\{\frac{2i\pi r r_1}{\lambda_p \zeta}\cos(\phi_1 - \phi_2)\right\} r_1 dr_1 d\phi_1 \tag{1}$$

where $\zeta = L - z$, λ_p, λ_e are probe and excitation beam wavelengths respectively, $(r_1, \phi_1), (r, \phi_2)$ are polar coordinates at sample and detector planes, respectivelly and $U_i(r, z, t)$ is the probe beam field amplitude with additional phase arising from the TL effect. In order to solve Eq. (1), Bessel function of zeroth-order is introduced using the following property

$$\int_0^{2\pi} exp\left\{\frac{2i\pi r r_1}{\lambda_p \zeta}\cos(\phi_1 - \phi_2)\right\} d\phi_1 = 2\pi J_0\left(\frac{2\pi r r_1}{\lambda_p \zeta}\right) \tag{2}$$

Using Eq. (2), the expression of Eq. (1) can be further simplified. The probe beam electric field amplitude at the detector plane takes the following form

$$U(r, z, t) = \frac{i}{\zeta \lambda_p} 2\pi \exp\left\{\frac{-2i\pi}{\lambda_p}\left(\zeta + \frac{r^2}{2\zeta}\right)\right\} \int_0^\infty U_i(r_1, z, t)$$
$$J_0\left(\frac{2\pi r_1 r}{\lambda_p \zeta}\right) \exp\left\{\frac{-i\pi}{\lambda_p}\frac{r_1^2}{\zeta}\right\} r_1 dr_1 \tag{3}$$

The initial probe beam electric field amplitude $U_i(r_1, z, t)$ in Eq. (3) can be defined as the product of the probe beam electric field amplitude without TL effect $|U_i|$ and an exponential phase factor introduced by the TL effect; $\exp\{-i\frac{\pi}{\lambda_p}(\frac{r_1^2}{R} + 2\Phi(r_1, z, t))\}$. Here $\Phi(r_1, z, t)$ is the phase shift on the probe beam wavefront due to the temperature gradient,

$$(2\pi/\lambda_p)\Phi(r, z, t) = (2\pi/\lambda_p)l\frac{dn}{dT}\{\Delta T(r, z, t) - \Delta T(r, 0, t)\} \tag{4}$$

where l is the thickness of the sample, $\Delta T(r, z, t)$ is the temperature change, dn/dT is the refractive index gradient and R is the radius of curvature. For a Gaussian beam passing through a very narrow region, we can use the approximation $R \gg r_1$. For a Gaussian excitation beam an expression for $\Phi(r_1, z, t)$ can be obtained from non-steady state heat diffusion equation as [11];

$$\Phi(g, z, t) = -\frac{\Phi_0}{2}\int_{t'}^1 \frac{\{1 - \exp(-2m(z)g)\tau\}}{\tau} d\tau \tag{5}$$

$$\Phi_0 = \frac{\alpha l P_e dn/dT}{\kappa \lambda_p} \tag{6}$$

where $t' = 1/(1 + 2t/t_c(z))$. P_e is the excitation beam power, κ is thermal conductivity and α is the absorption coefficient of the sample. Additionally we have introduced two parameters $g = (\frac{r_1^2}{\omega_p^2})$ and $m = (\frac{\omega_p}{\omega_e})^2$ which define the degree of mismatching between

probe and excitation beams. Assuming $\Phi \ll 1$ we can ignore higher order terms in expansion of phase factor i.e. $\exp\{-i(2\pi/\lambda_p)\Phi\} \approx (1 - i2\pi\Phi/\lambda_p)$. Thus Eq. (3) takes the following form

$$U(r, z, t) = B(z, r) \int_0^\infty \exp\{-g - iv(z)g\}(1-i\Phi)$$
$$J_0\left(r\sqrt{g}\eta(z)\right)dg \tag{7}$$

The parameters in Eq. (7) are defined as follows,

$$\eta(z) = 2\pi\omega_p(z)/\lambda_p\zeta$$
$$v(z) = (z - a_p)/z_p + (z_p/\zeta)[1 + (z - a_p)^2/z_p^2]$$
$$\omega_{p,e} = \omega_{op,oe}\sqrt{1 + (z - a_{p,e})^2/z_{p,e}^2} \tag{8}$$
$$B(z, r) = i\omega_p(z)(\sqrt{2\pi P_p/\lambda_p\zeta})\exp[-i(\pi/\lambda_p)$$
$$\times (2\zeta + r^2/\zeta) + i\arctan(z/z_p)]$$

Here $z_{p,e} = \sqrt{\pi\omega_{op,oe}/\lambda_{p,e}}$ and a_p, a_e are their Rayleigh parameters and waist positions of the beams, whereas ω_{op} and ω_{oe} the radii at the waist, of the probe and the pump beams respectively. Integration over g in Eq. (7) can be done analytically using the following integral,

$$\int_0^\infty \exp\left\{-\left(1 + iv(z) + 2m(z)\tau\right)g\right\}J_0\left\{r\sqrt{g}\eta(z)\right\}dg$$
$$= \frac{1}{\sqrt{(1 + 2m(z)\tau)^2 + v(z)^2}}\exp\left\{\frac{r^2\eta(z)^2}{4((1 + 2m(z)\tau)^2 + v(z)^2)}\right.$$
$$\times (-(1 + 2m(z)\tau) + iv(z)) + i\arctan\left\{-\frac{v(z)}{1 + 2m(z)\tau}\right\}\bigg\} \tag{9}$$

We define new variables as:

$$M_0(z, \tau) = \frac{1}{\sqrt{(1 + 2m(z)\tau)^2 + v(z)^2}}$$
$$M_1(z, \tau) = \frac{1 + 2m(z)\tau}{4((1 + 2m(z)\tau)^2 + v(z)^2)}$$
$$M_2(z, \tau) = \frac{v}{4((1 + 2m(z)\tau)^2 + v(z)^2)} \tag{10}$$
$$M_3(z, \tau) = \arctan\left\{-\frac{v(z)}{1 + 2m(z)\tau}\right\}$$
$$M_4(z, \tau) = \sqrt{(M_1(z, 0) + M_1(z, \tau))^2 + (M_2(z, 0) - M_2(z, \tau))^2}$$

We can rewrite Eq. (9) in terms of the new variables in Eq. (10)

$$M(z, r, \tau) = M_0(z, \tau)\exp(-r^2 M_1(z, \tau)\eta(z)^2)$$
$$\exp\left(i[r^2\eta(z)^2 M_2(z, \tau) + M_3(z, \tau)]\right) \tag{11}$$

Using Eqs. (5) and (11), the probe beam electric field amplitude at the detector plane in Eq. (7) can be simplified as follows,

$$U(r, z, t) = B(z, r)\left\{M(z, r, 0) + i\frac{\Phi_0}{2}\int_{t'}^1 [M(z, r, 0)\right.$$
$$- M(z, r, \tau)]\frac{d\tau}{\tau}\bigg\} \tag{12}$$

The probe beam transmission intensity through ρ_0 is defined as

$$T(z, t) = \int_0^{\rho_0} |U(r, z, t)|^2 2\pi r\, dr \tag{13}$$

The TL signal is defined as the relative change of the probe beam transmission when the aperture is located in far field [12]

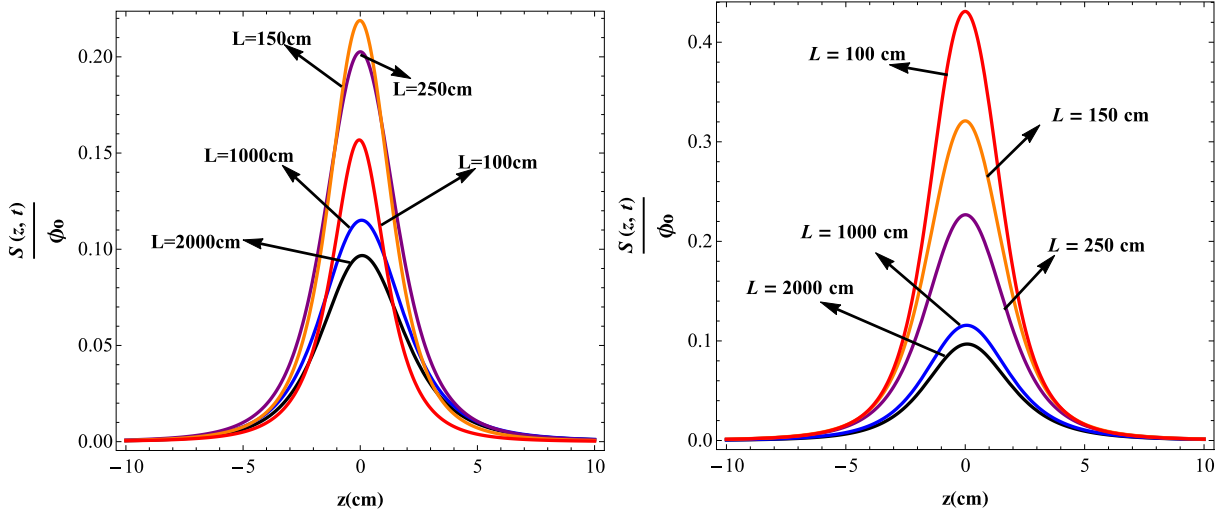$$S(z, t) = \frac{T(z, t) - T(0)}{T(0)} \tag{14}$$

Fig. 2. Z-scan signal obtained from Eq. (15) Fig. 2(a), Eq. (16) Fig. 2(b) in mode-mismatched scheme for various values of L. The parameters are $z_p = 70$ cm, $z_e = 0.05$ cm, $a_p = -20$, $a_e = 0$, $D = 1.431 \times 10^{-3} \frac{cm^2}{s}$, $\rho_0 = 0.1$ cm $\omega_{p0} = 0.038$ cm and $\omega_{e0} = 0.001$ cm, $t = 0.0714$ s.

where $T(0)$ is the value of T(z,t) for $\Phi = 0$. After integration over r the expression for S(z,t) as a function of the sample position is calculated as follows

$$
S(z,t) = \int_{t'}^{1} \frac{2M_1(z,0)M_0(z,\tau)\phi_0}{(1 - \exp\{-2\rho_0^2 M_1(z,0)y^2\})M_0(z,0)M_4(z,\tau)} \frac{d\tau}{\tau}
$$

$$
\left[\sin\left\{ \arctan\left[\frac{M_2(z,0) - M_2(z,\tau)}{M_1(z,0) + M_1(z,\tau)} \right] + M_3(z,0) - M_3(z,\tau) \right\} \right.
$$

$$
- \exp\{-2\rho_0^2(M_1(z,0) + M_1(z,\tau)y^2)\} \sin\left\{ \arctan\left[\frac{M_2(z,0) - M_2(z,\tau)}{M_1(z,0) + M_1(z,\tau)} \right] \right.
$$

$$
\left. \left. + \rho_0^2 y^2(M_2(z,0) - M_2(z,\tau)) + M_3(z,0) - M_3(z,\tau) \right\} \right]
$$

(15)

Apart from the dependence on the sample position, the TL signal in Eq. (15) depends on the aperture size ρ_0 as well. This dependence can be conveniently ignored when the aperture size is much smaller than the probe beam radius at the detector plane. This situation can be reached for larger values of L; however, in real situation the distance L is small (100 cm) and the dependence on ρ_0 must be considered. In the situation when the contribution of ρ_0 is ignored, the TL signal can be described by a simple expression as Eq.(42) of [11] or Eq. (23) of [12].

$$
S(z,t) = \Phi_0 \arctan\left\{ \frac{4m(z)v(z)t/t_c(z)}{v(z)^2 + (1 + 2m(z))^2 + (1 + 2m(z) + v(z)^2)2t/t_c(z)} \right\}
$$

(16)

The expression in Eq. (15) is similar to the one derived by Marcano et al. [12] (see Eq. 20, 21 and Eq. 22); However our calculations reveal three different issues; (i) the exponential in the second term of the numerator of Eq. (21) [12] is incomplete, the correct form of the exponent should be $\exp[-\{F(z,t) + F(0,t)\}Y(z)^2r_0^2]$; (ii) the sign of the term $-\eta(z,0) + \eta(z,t)$ in Eq. (22) is inconsistent with our calculations, the correct form is $\eta(z,0) - \eta(z,t)$; (iii) Eq. (23) [12] or Eq. (42) of [11] ignores the ρ_0 dependence, but it must be considered for small values of L. The dependence of the TL signal on ρ_0 and L can be analyzed using Eqs. (15) and (16) and comparing the results.

In Figs. 2(a) and 2(b), we plot the TL Z-scan signals obtained from Eqs. (15) and (16) in mode-mismatched scheme for various detector positions. For $L = 1000$ cm and $L = 2000$ cm the TL signals are identical. The TL signal calculated with Eq. (15) is smaller than the TL signal calculated using Eq. (16) for smaller values of L. For example in the case of $L = 100$ cm, the maximum signal of Fig. 2(a) is only 23% of the signal peak of Fig. 2(b). This result indicates that there is a strong dependence of the TL signal with L, contrary to the situation when ρ_0 contribution was ignored in case of Eq. (16) in [12] and Eq. (42) of [11]. As seen in Fig. 2(a) the peak value of the TL signal shows interesting dependence on L. To illustrate this dependence we plot the Z-scan signal at $z = 0$ as a function of L at different times as shown in Fig. 3.

In Fig. 3 we see that $S(0,t)$ increases when L increases, reaching a maximum value, and afterwards begins to decrease when detector position moves further away. This behavior is not observed in the inset of Fig. 3 where $S(0,t)$ reaches its maximum with shorter values of L and decreases afterwards as we increase L. In Fig. 4(a) the dependence of the signal on different Rayleigh parameters is shown. The results show that, the signal is nearly independent on the probe beam Rayleigh parameter z_p. We show the calculation of the TL signal for $z_e = 0.05$ cm and zp = 200, 2000, 5000, 10 000 cm, as indicated. The rest of the parameters are as in Fig. 2. In Fig. 4(b), the dependence of the TL signal are plotted using Eq. (16) for same parameters.
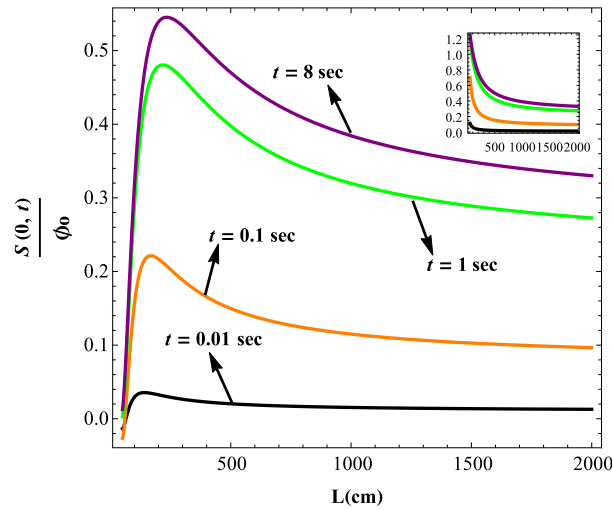
Fig. 3. Dependence of the TL signal peak at $z = 0$ versus L at different times for Eq. (15). The inset of the figure corresponds to Eq. (16). The rest of parameters are $z_p = 70$ cm, $z_e = 0.05$ cm, $a_p = -20$, $a_e = 0$, $D = 1.431 \times 10^{-3} \frac{cm^2}{s}$, $\rho_0 = 0.1$ cm $\omega_{p0} = 0.038$ and $\omega_{e0} = 0.001$. The origin of horizontal scale is set at L = 50 cm.
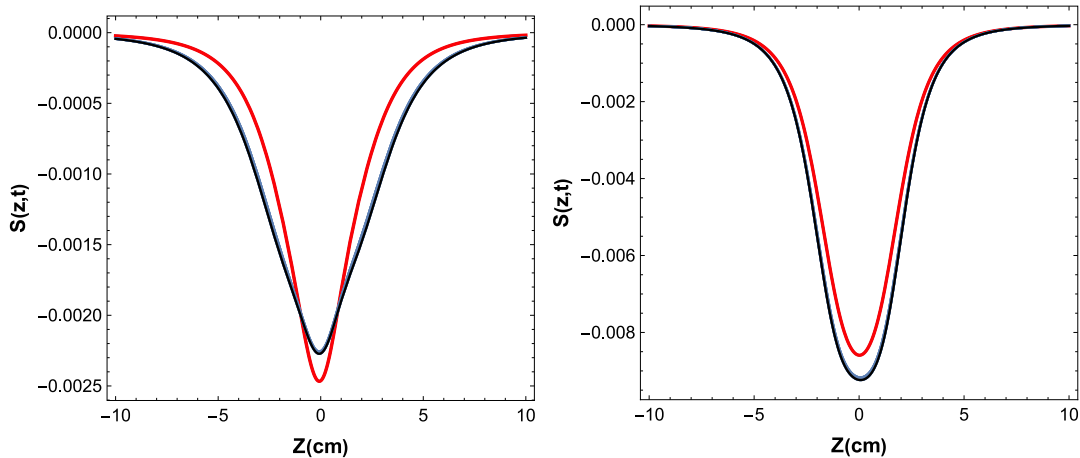

Fig. 4. Fig. 4(a) is the Z-scan calculated from Eq. (15) for different values of the probe beam Rayleigh parameters. The Rayleigh parameter of the excitation beam is ze = 0.05 cm. The values of ($z_p = 200$, $z_p = 2000$, $z_p = 50000$, $z_p = 10000$) are shown in red, blue, purple and black respectively. Detector to sample position L is set at 100 cm, while the rest of parameters are the same as in Fig. 2. Fig. 4(b) shows the Z-scan for same parameters using Eq. (16). The value of ϕ_0 is -0.013. (For interpretation of the references to color in this figure legend, the reader is referred to the web version of this article.)

3. Experimental part

In order to validate the presented modified model, we calculate the absorption coefficient and the thermal diffusivity of water using the experimental setup shown in Fig. 5. As a probe beam we used a 2 mW He–Ne laser (05-UR-111, Melles Griot) collimated by a set of lenses L3 (LB1027-A, f = 40 mm, Thorlabs) and L4 (LB1676-A, f = 100 mm, Thorlabs), respectively. The distance between lenses was adjusted in order to change the Rayleigh parameter of the probe beam. A 532 nm diode-pumped solid state laser (DPSS) (MGL-III- 532 nm-1000, UltraLasers) was used as the excitation light which was intensity modulated at 7 Hz using a signal generator (SG) (Rigol DG 2041 A, Batronix). A collimation system with lens L1 (LB1027-A, f = 40 mm, Thorlabs) and L2 (LB1676-A, f = 100 mm, Thorlabs) generated a 3 mm collimated excitation beam which was focused onto the sample by lens L3 (LB1676-A, f = 100 mm, Thorlabs).

The radius of the excitation beam (10 μm) was measured using a commercial dual scanning slit beam profiler (BP209-VISM, Thorlabs). The Silicon detector (PDA 36A-EC, Thorlabs) converted the intensity changes of the probe beam through a 1 mm pinhole (encapsulated in detector) into analog voltage. The interference filter 632.8 nm (MELLES GRIOT) removed any residual light at 532 nm.

For a 2 mm cell, L = 100 cm and 650 mW power we measured the TL signal for different positions of sample cell (Z-scan measurement) as shown in (Fig. 6(a)) for Z = 0. Additionally, we performed fitting on Z-scan measurement (Fig. 6(b)) and (Fig. 6(c))
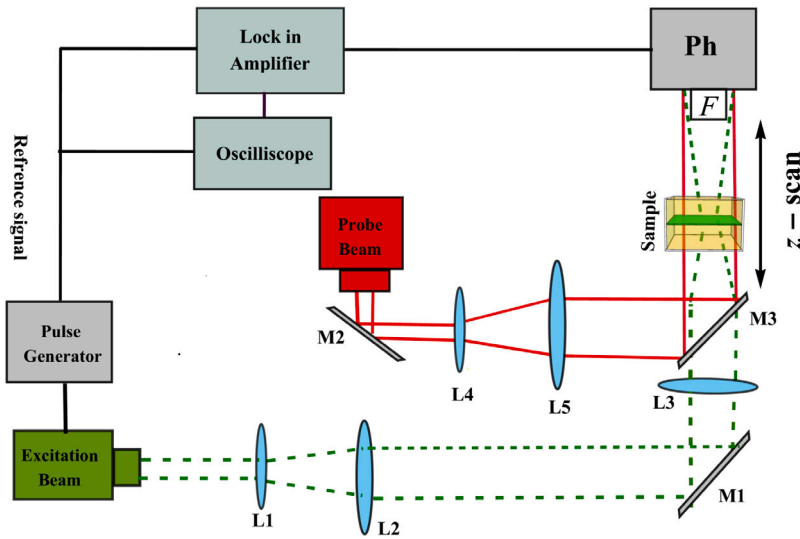
Fig. 5. Experimental configuration of the pump-probe TL setup. Ph: photodetector; L1–L5: lenses; M1–M2: turning mirrors, M3: dichroic mirror, F: filter.
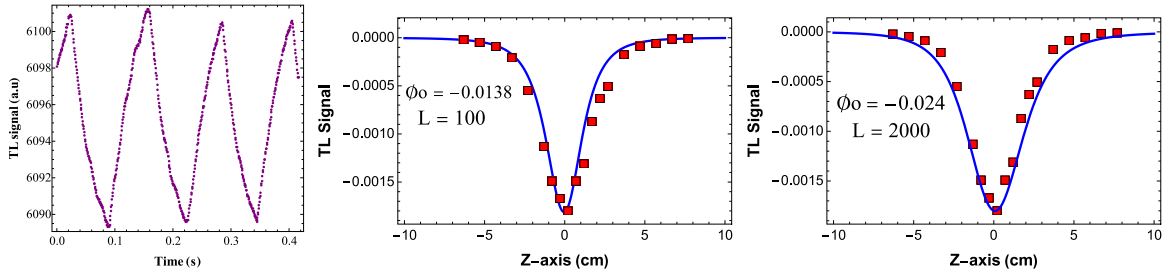

Fig. 6. (a) TL signal obtained from digital oscilloscope (b)–(c) Mode-mismatched curve fit of experimental data points with Eqs. (15) and (16), respectively: The parameters used for curve fit $z_p = 70$ cm, $z_e = 0.05$ cm, $a_p = -20$, $a_e = 0$, $D = 1.431 \times 10^{-3}$ $\frac{cm^2}{s}$, $\omega_{p0} = 0.038$ cm and $\omega_{e0} = 0.001$ cm, t = 0.0714 s.

using Eqs. (15) and (16) respectively. Considering ϕ_0 and D as adjustable parameters [13] we got $\phi_0 = -0.013$ and $D = 1.43 \times 10^{-3}$ from the curve fit in first case whereas for the later, we obtain $\phi_0 = -0.024$. Using the photothermal parameters of water: $dn/dT = 0.91 \times 10^{-4}$ K^{-1}, $\kappa = 5.98 \times 10^{-3}$ W/cm K, $Pe = 650$ mW and $\lambda_p = 632.8$ nm, the value of absorption coefficient can be obtained from Eq. (6) which gives a value of $\alpha = 4.16 \times 10^{-4}$ cm^{-1}. The obtained results for α and D match pretty well with previously reported values [3,14].

As indicated in the caption of (Fig. 6(b)), the fitting was performed using the experimental value of L. However, for the fitting performed with Eq. (16) in (Fig. 6(c)), the value of L was adjusted to a very large value ($L = 2000$ cm) which does not match the real experimental situation and is inconsistent. Similarly, this is in agreement with the measurement performed in the Ref. [12] in which L was also adjusted to a large value. Collectively, these results demonstrate the significance of the pinhole size and its correlation with L. In addition, indicate the validity of the proposed modified TL model for which L takes logical values in agreement with the experimental ones.

4. Conclusion

We presented a modified TL model for Z-scan measurement, which describes more precisely the behavior of the TL signal under different experimental situations. Furthermore, we show the feasibility of using the generalized model for different experimental configurations including small and large values of L. The theory enables to perform fitting on the experimental data using the values of Φ_0 and D as fitting parameters and there is a pretty well agreement between the values of L both in theory and experiment. To test the validity of our model, we performed mode-mismatched Z-scan experiment using double distilled and deionized water as a sample. The obtained values for the absorption coefficient and thermal diffusivity match pretty well with the literature values.

Declaration of competing interest

The authors declare that they have no known competing financial interests or personal relationships that could have appeared to influence the work reported in this paper.

Acknowledgments

References

[1] H. Cabrera, A. Marcano, Y. Castellanos, Condens. Matter Phys. 9 (2006) 385–389.
[2] A.M. O., H. Maillotte, D. Gindre, D. Métin, Opt. Lett. 21 (2) (1996) 101–103.
[3] A. Marcano, H. Cabrera, M. Guerra, R.A. Cruz, C. Jacinto, T. Catunda, J. Opt. Soc. Amer. B 23 (7) (2006) 1408–1413.
[4] R. Leite, R. Moore, J. Whinnery, Appl. Phys. Lett. 5 (7) (1964) 141–143.
[5] D. Solominini, J. Appl. Phys. 37 (1965) 3314–3315.
[6] A. Rahman, H. Cabrera, M.U. Malik, I. Ashraf, J. Opt. Soc. Amer. B 38 (1) (2021) 52–59.
[7] J. Shen, A.J. Soroka, R.D. Snook, J. Appl. Phys. 78 (2) (1995) 700–708.
[8] S.E. Bialkowski, Photothermal Spectroscopy Methods for Chemical Analysis, Vol. 177, John Wiley & Sons, 1996.
[9] S. Sankararaman, Optik 248 (2021) 168–176.
[10] K. Dobek, Appl. Phys. B 128 (2) (2022) 1–21.
[11] J. Shen, R.D. Lowe, R.D. Snook, Chem. Phys. 165 (2–3) (1992) 385–396.
[12] A. Marcano, C. Loper, N. Melikechi, J. Opt. Soc. Amer. B 19 (1) (2002) 119–124.
[13] P. Pedreira, L. Hirsch, J. Pereira, A. Medina, A. Bento, M. Baesso, Rev. Sci. Instrum. 74 (1) (2003) 808–810.
[14] R.M. Pope, E.S. Fry, Appl. Opt. 36 (33) (1997) 8710–8723.